Photothermal induced defect engineering: boosting photothermal synergistic selective catalysis oxidation of benzyl alcohol over in-situ oxygen vacancy modulated ultrathin ZnTi-LDH nanosheet

Wen Ma,[a] Tao Li,[a] Jia-Hao Gao,[a] Ren-Tian Zhang,[a] Peng Wang,[a] Qi Chen,[c] Hong-Zi Tan,[d] Jian-Feng Diao,[e] Kai-Qiang Jing,*[a,b] Zhong-Ning Xu,*[b] Ling Wu*[c]

[a]School of Materials and Chemical Engineering, Xuzhou University of Technology, Xuzhou, Jiangsu 221018, China

[b]State Key Laboratory of Structural Chemistry, Fujian Institute of Research on the Structure of Matter, Chinese Academy of Sciences, Fuzhou, Fujian 35000, China

[c]State Key Laboratory of Photocatalysis on Energy and Environment, College of Chemistry, Fuzhou University, Fuzhou 350116, China

[d]School of Chemistry & Chemical Engineering, Shandong University of Technology, Zibo, Shandong 255049, China

[e]School of Chemistry and Chemical Engineering, Linyi University, Linyi, Shandong 276005, China

*Corresponding authors

E-mail address:

wuling@fzu.edu.cn (L. Wu). znxu@fjirsm.ac.cn (Z-N. Xu). jingkaiqiang@xzit.edu.cn (K-Q. Jing).

1. Reagents and chemicals

Zinc nitrate hexahydrate (Zn $(NO_3)_2 \cdot 6H_2O$) was obtained by Sinopharm Chemical Reagent Co., Ltd. (Shanghai, China). Urea (CH_4N_2O, 99%), Titanium (IV) Chloride ($TiCl_4$, 99%), Benzyl alcohol (BA, 99%), Benzaldehyde (BAD, 99%), Acetonitrile (99.9%), Ethanol was purchased by Adamas. Deionized water was also utilized.

2. Characterization of the prepared ZnTi-LDH sample and the calculated formula

The X-ray diffraction (XRD) was analyzed by utilizing a Rigaku Ultima IV X-ray diffractometer within the scope of 5°-80°. The Fourier transform Infrared (FT-IR) spectra were obtained using an ALPHA instrument from Bruker, Germany. The Shimadzu 3600-plus was utilized to perform UV-visible diffuse reflectance spectroscopy (UV-vis DRS, 200-800 nm) at the treated temperature under 25, 50 and 70 °C. The X-ray photoelectron spectra (XPS) were performed on an Thermo ESCALAB 250Xi with monochromatic Al Ka Radiation (E = 1486.2 eV) at 3.0×10^{-10} mbar. The XPS spectral analysis related to referencing C 1 s was 284.8 eV, which corrected specimens charging. Transmission electron microscopy (TEM), higher-resolution transmission electron microscopy (HRTEM) and the High Angle Annular Dark Field Scanning Transmission Electron Microscopy (HAADF-STEM) were taken using JEM-F200 microscope at an accelerating voltage of 200 kV. The HAADF-STEM EDS mapping was recorded on Ultim Max 80. The Agilent 5500 was used to record the thickness of samples. To conduct the AFM experiment, samples were first dispersed in ethanol via ultrasonic bath treatment for 10 minutes, followed by dilution in ethanol. Subsequently, a droplet of the diluted dispersion was deposited onto a freshly cleaved mica surface and allowed to dry in ambient conditions. This procedure was employed to assess the morphology of the resulting nanosheets on the mica substrate. The oxygen vacancies were measured via electron paramagnetic resonance (EPR, Brucker A300). Before carrying out experiment, 100 mg ZnTi-LDH catalyst was put into the paramagnetic tube. Whereafter, the EPR signals were recorded at 25, 50 and 70 °C. The nuclear magnetic resonance of hydrogen spectrum (^{1}H NMR) was measured on the Bruker AVANCE NEO 400MHZ. Photoluminescence (PL) and Time-resolved transient

photoluminescence (TRPL) spectra were measured by FLS-1000, Edinburgh Instruments Ltd. Decay curves were analyzed at the excitation of 380 nm for the ZnTi-LDH under emission of 495 nm. Before starting experiment, the chamber was treated at 25 °C, 50 °C and 70 °C, respectively.

2.1 The calculated methods and formula

We adopted the external method to determine the concentration of BA and BAD. We adopted 0.1 mmoL, 0.05 mmoL, 0.025 mmoL and 0.0125 mmoL BA dissolving into chromatography bottle with 1.5 mL acetonitrile, respectively. Subsequently, we extracted 1μL the above solution via automatic sampler, and then analyzed the retention time and peak area of BA via gas chromatograph (A60, PANNA) with automatic sampler. Similarly, the concentration of BAD was confirmed via the above steps except changing BA into BAD. Ultimately, we plotted the standard curves for benzyl alcohol and benzaldehyde, respectively, by measuring the concentrations at four points.

The calculated formula named the percent conversion of BA and percent selectivity for BAD were described as follows:

Conversion (%) = $[(C_0 - C_{BA})/C_0] \times 100\%$; Selectivity (%) = $[C_{BAD} / (C_0 - C_{BA})] \times 100\%$

The C_0 is the original concentration of BA, and C_{BA} is the concentration of benzyl alcohol as a substrate after the reaction. The C_{BAD} is the concentration of corresponding BAD.

3. The Density functional theory (DFT) calculations

All the DFT calculations were performed based on the Vienna Ab-inito Simulation Package (VASP)[1,2]. The exchange-correlation effects were described by the Perdew-Burke-Ernzerhof (PBE) functional within the generalized gradient approximation (GGA) method[3,4]. The core-valence interactions were accounted by the projected augmented wave (PAW) method[5]. The energy cutoff for plane wave expansions was set to 400 eV, and the 3×3×1 Monkhorst-Pack grid k-points were selected to sample the Brillouin zone integration. The structural optimization was completed for energy

and force convergence set at 1.0×10^{-4} eV and 0.05 eV $Å^{-1}$, respectively.

The adsorption energies (E_{ads}) of Ph-CH_2OH are calculated by

$E_{ads} = E_{*Ph\text{-}CH2OH} - E_{Ph\text{-}CH2OH} - E_{sub}$

where $E_{*Ph\text{-}CH2OH}$ represents the energy after the adsorption of Ph-CH_2OH on the substrates. $E_{Ph\text{-}CH2OH}$ is the energy of the Ph-CH_2OH. E_{sub} is the energy of ZnTi-LDH and ZnTi-LDH-OVs surfaces.

The Gibbs free energy change (ΔG) of each step is calculated using the following formula:

$$\Delta G = \Delta E + \Delta ZPE - T\Delta S$$

where ΔE is the electronic energy difference directly obtained from DFT calculations, ΔZPE is the zero point energy difference, T is the room temperature (298.15 K) and ΔS is the entropy change. ZPE could be obtained after frequency calculation by[6]:

$$ZPE = \frac{1}{2}\sum hvi$$

4. Electrochemistry measurement

The electrochemical analysis was conducted on CHI 660E Chenhua Instrument Company through a traditional three electrode cell, which utilized reference electrode, a Pt plate and the counter electrode Ag/AgCl electrode. The electrolyte consisted of a 0.2 M Na_2SO_4 aqueous solution without any additives (pH = 6.8). The working electrode was fabricated on indium-tin oxide (ITO) glass, which was cleaned by ultrasonicating in ethanol for two hours and subsequently dried at 353 K. The perimeter of the ITO glass was protected using Scotch tape. Five milligrams of the sample were dispersed in 0.5 mL of ethanol via sonication to form a slurry. This slurry was then uniformly spread onto the pre-treated ITO glass substrate. Following air drying, the working electrode was further dried at 393 K for two hours to enhance adhesion. Before performing every electrochemical measurement, we set the heater temperature as 25 °C, 50 °C and 70 °C to heat electrolyte until the target temperature.

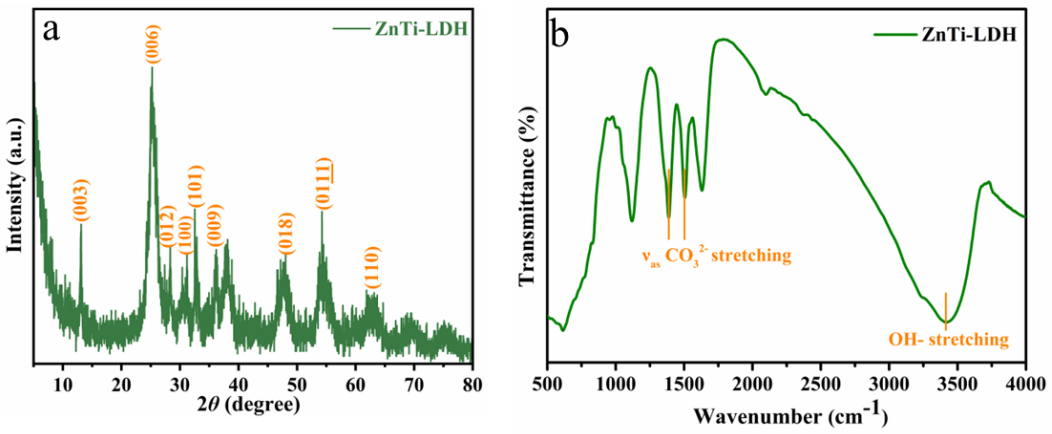

Fig. S1 Characterizations of the ZnTi-LDH sample. (a) XRD; (b) FTIR.

The FTIR was performed to investigate the chemical structure. In Fig. S1b, the wide peak at 3417 cm^{-1} for the ZnTi-LDH can be assigned to OH group. The two peaks at 1384 and 1510 cm^{-1} for the ZnTi-LDH can be attributed to carbonate ions (CO_3^{2-}), indicating that the interlayer anions are CO_3^{2-}. This result indicates that the ZnTi-LDH sample can be synthesized successfully.

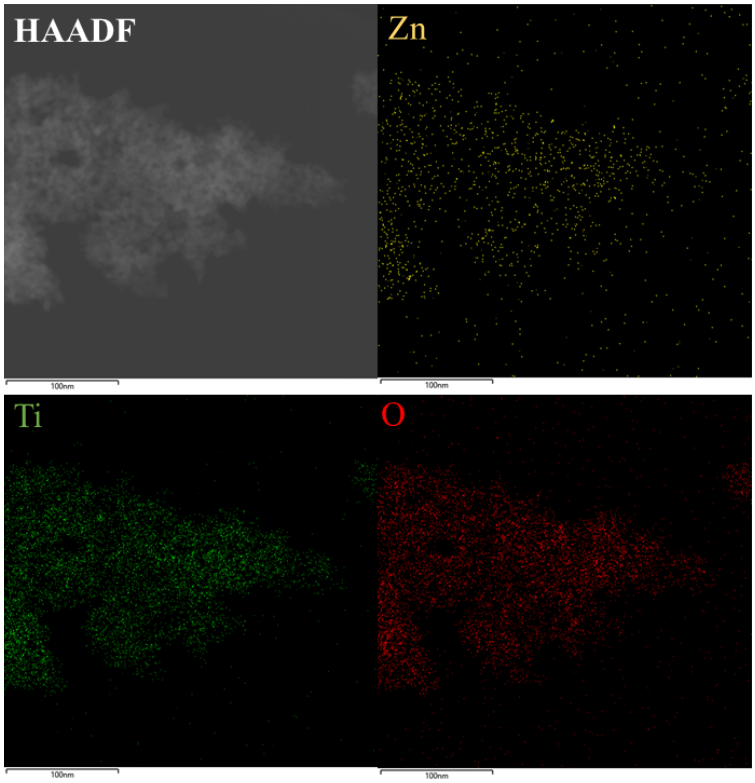

Fig. S2 HAADF-STEM images of the ZnTi-LDH nanosheets and the corresponding element mapping.

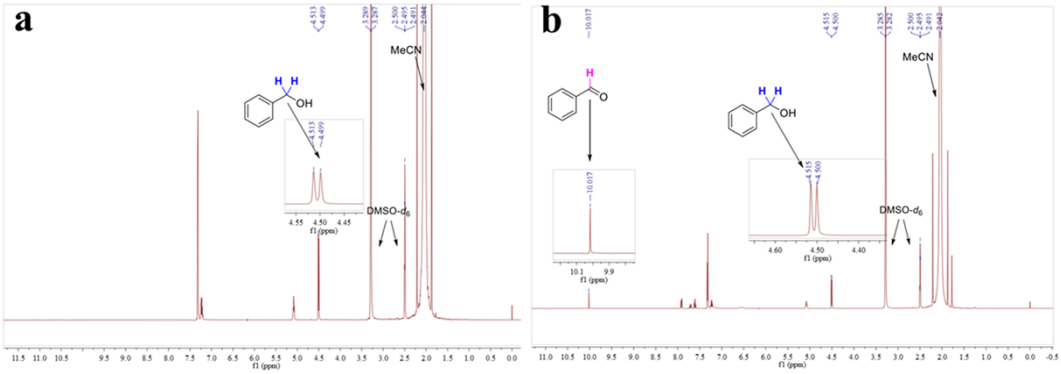

Fig. S3 ^{1}H NMR spectra. (a) The BA (C_7H_8O) and Acetonitrile (MeCN); (b) The BA, BAD (C_7H_6O) and Acetonitrile after 4 hours of reaction at 25 °C reactive temperature.

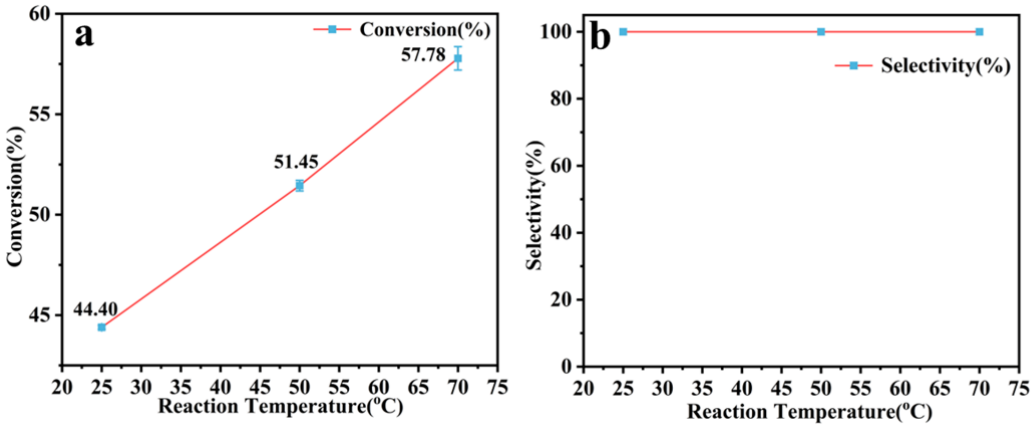

Fig. S4 The conversion of BA (a) and the selectivity of BAD (b) over the ZnTi-LDH sample under 25, 50 and 70 °C reactive temperature. Reaction conditions: ZnTi-LDH: 20 mg; BA: 0.1 mmol; Acetonitrile: 1.5 mL; O_2: 1 atm, λ≥400 nm; Reaction time: 4 h.

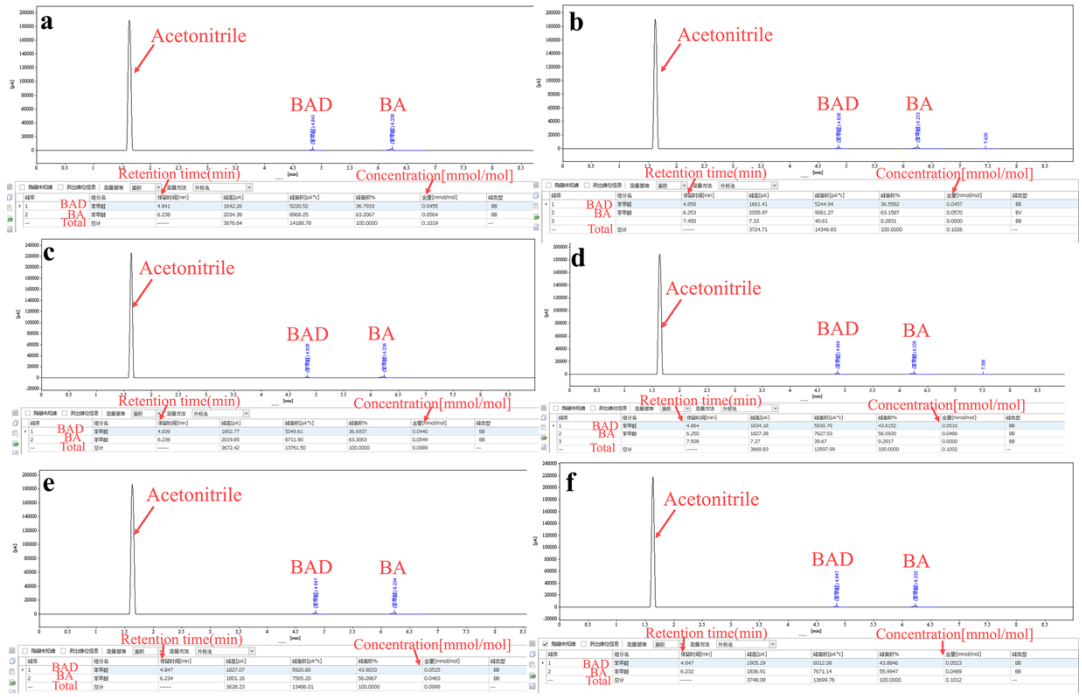

Fig. S5 Chromatographic analysis data for photothermal selective oxidation of BA over the ZnTi-LDH sample at 25 °C reactive temperature (a) The first collection; (b) Parallel second collection; (c) The third collection; At 50 °C reactive temperature (d) The first collection; (e) Parallel second collection; (f) The third collection.

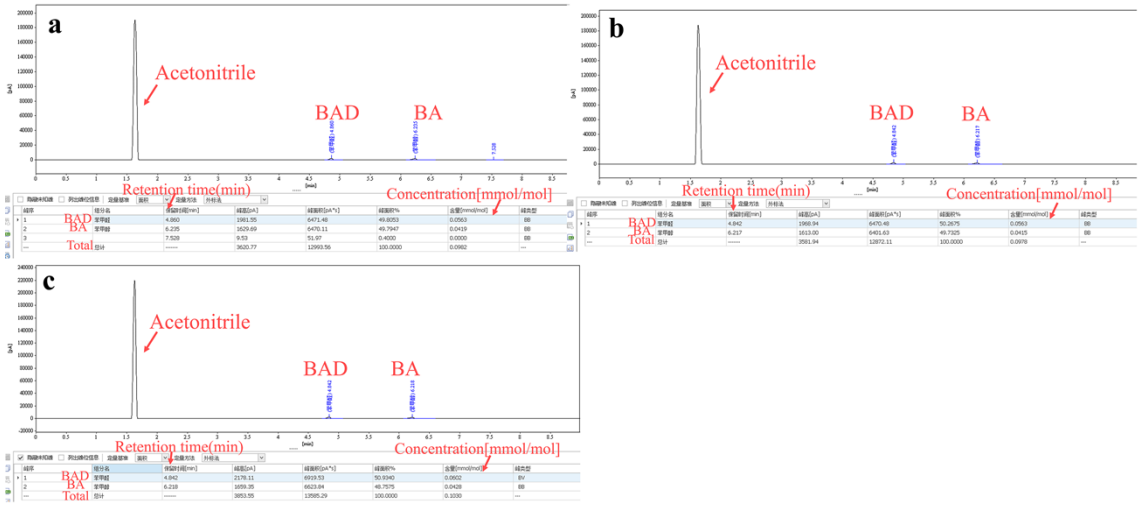

Fig. S6 Chromatographic analysis data for photothermal selective oxidation of BA over the ZnTi-LDH sample at 70 °C reactive temperature (a) The first collection; (b) Parallel second collection; (c) The third collection.

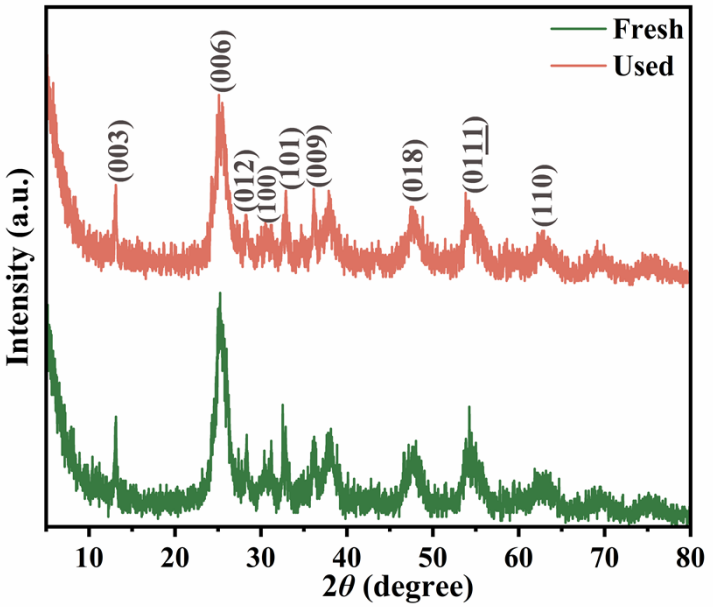

Fig. S7 The XRD patterns of the ZT-70 sample before the reaction and after three runs.

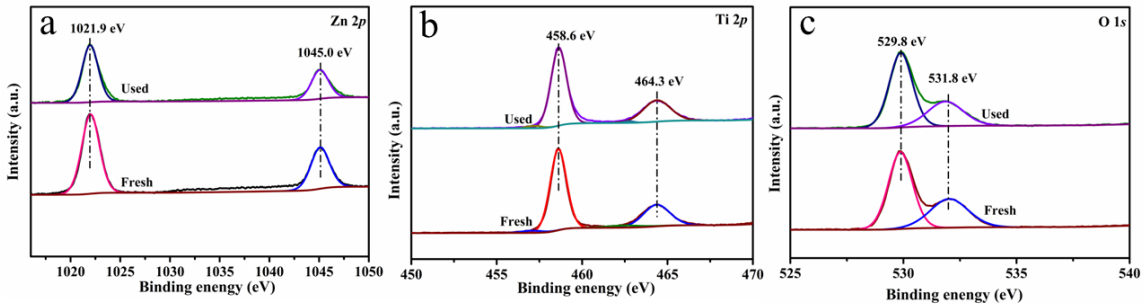

Fig. S8 The XPS spectra of the ZT-70 sample before the reaction and after three runs: (a) Zn 2*p*; (b) Ti 2*p*; (c) O 1*s*.

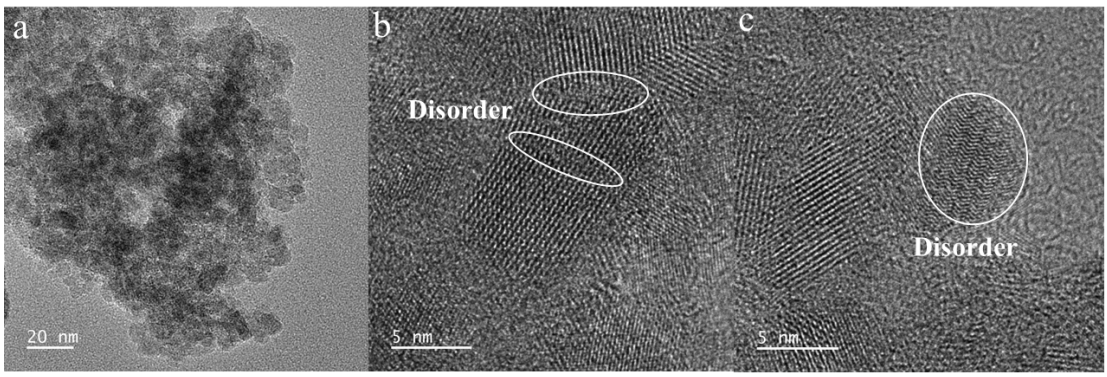

Fig. S9 The TEM image (a) and HRTEM images (b and c) of the ZT-70 sample after reaction via three runs.

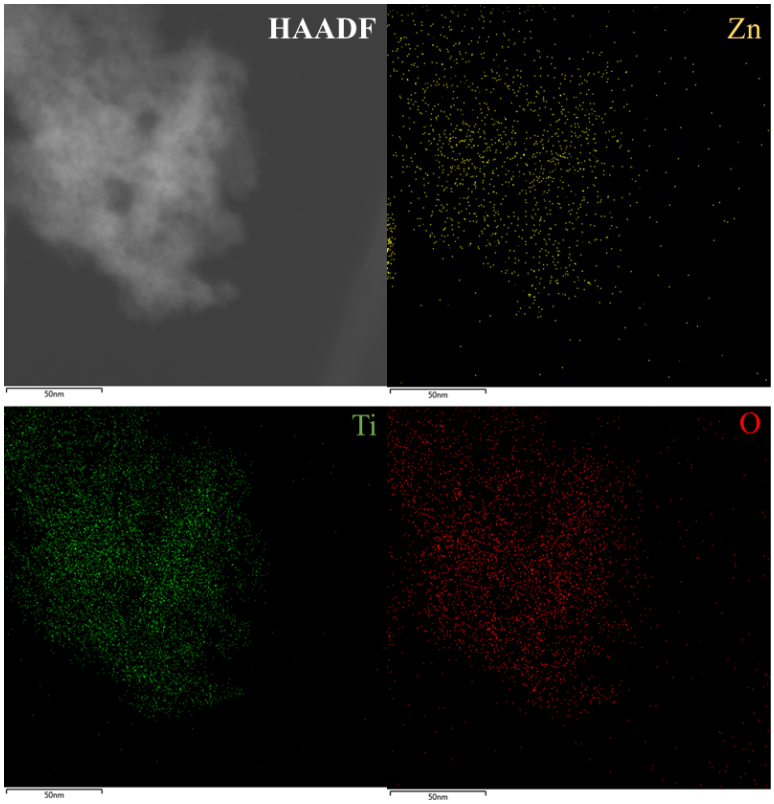

Fig. S10 The HAADF-STEM images of the ZT-70 sample after reaction via three runs and the corresponding element mapping.

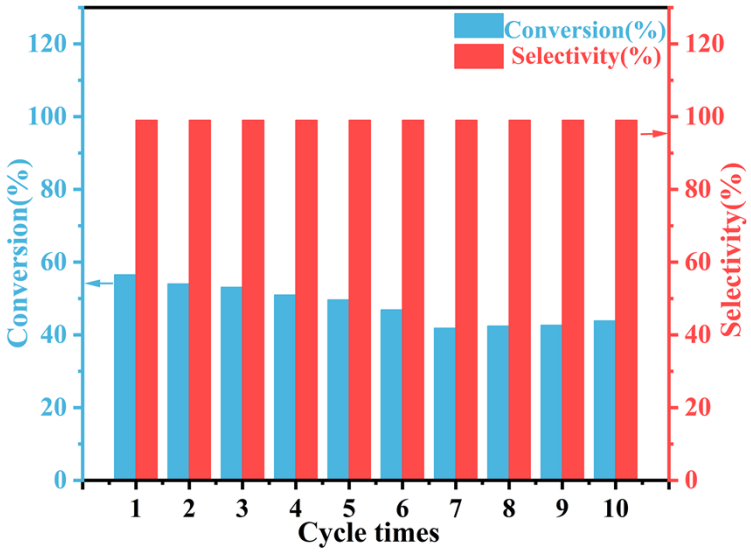

Fig. S11 Cyclic experiment of the photothermal selective oxidation of BA over the ZnTi-LDH sample at 70 °C reactive temperature. Reaction conditions: ZnTi-LDH: 20 milligrams; BA: 0.1 millimole; Acetonitrile: 1.5 milliliter; O_2: 1 atm, $\lambda \geq 400$ nm. Reaction time: 4 hours.

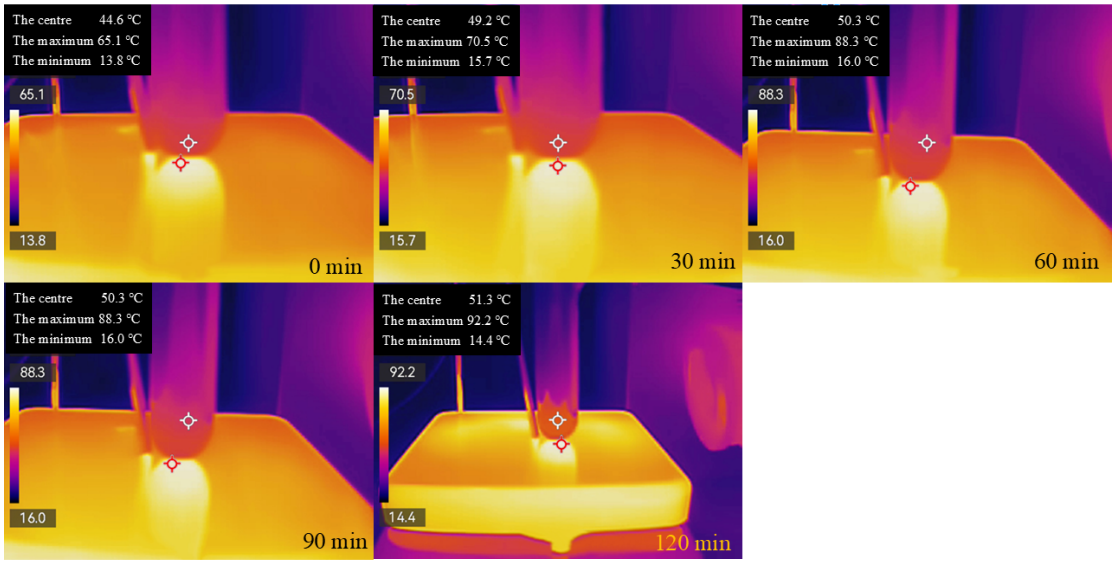

Fig. S12 Photothermal IR mapping images of the ZnTi-LDH sample under the reactive temperature at 50 °C in the solution during the reaction time from 0 to 120 minutes.

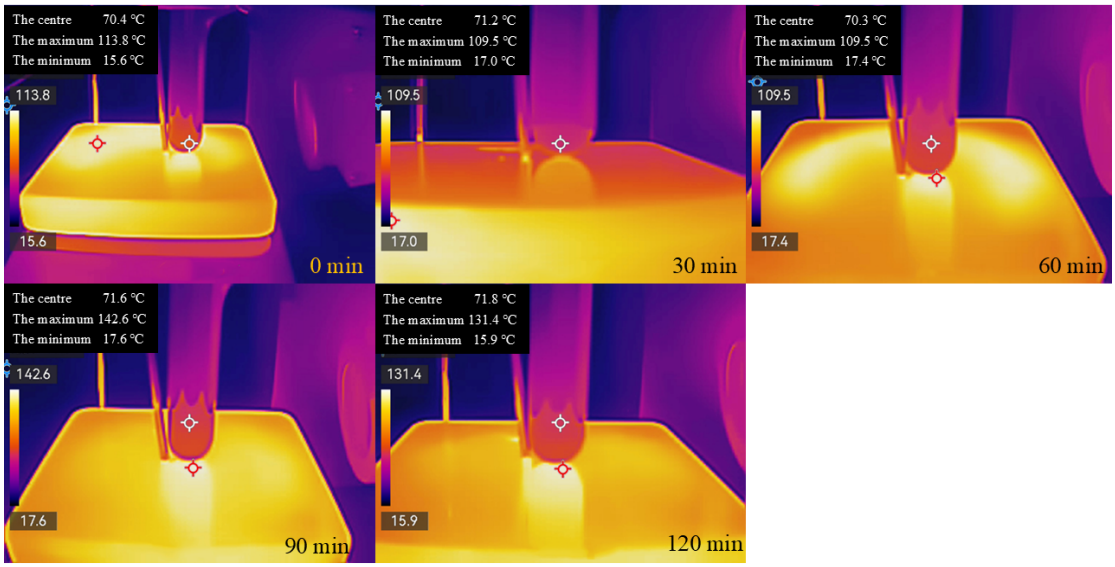

Fig. S13 Photothermal IR mapping images of the ZnTi-LDH sample under the reactive temperature at 70 °C in the solution during the reaction time from 0 to 120 minutes.

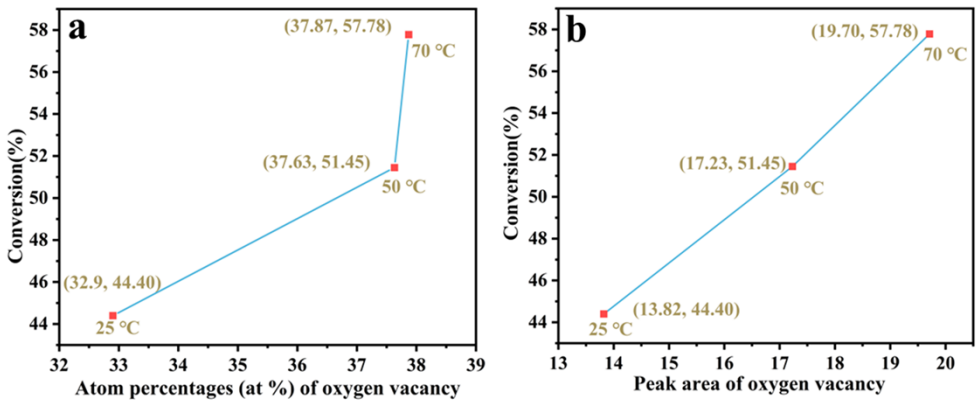

Fig. S14 (a) A quantitative correlation plot between the atom percentages of oxygen vacancy (from XPS) and conversion rate; (b) A quantitative correlation plot between the peak area of oxygen vacancy (from EPR) and conversion rate.

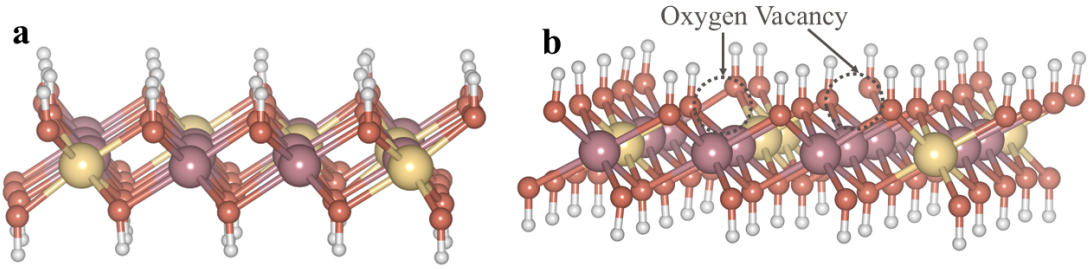

Fig. S15 The Density functional theory (DFT) calculation models: (a) ZnTi-LDH sample without oxygen vacancy; (b) ZnTi-LDH sample with oxygen vacancy.

Table S1: Photothermal synergy selective oxidation of benzyl alcohol over the ZnTi-LDH sample with (+) visible light. The thermocatalysis of the ZnTi-LDH sample without (-) visible light.

Entry	Sample	Reactive Temperature	Light	Atmosphere	Conversion（%）	Selectivity（%）
1	ZnTi-LDH[a]	70 °C	+	Air	37.7	99
2	ZnTi-LDH[a]	70 °C	+	N_2	4	99
3	ZnTi-LDH[a]	25 °C	-	O_2	0.6	99
4	ZnTi-LDH[a]	50 °C	-	O_2	0.44	99
5	ZnTi-LDH[a]	70 °C	-	O_2	0.43	99
6	-	70 °C	+	O_2	-	-

7	ZnTi-LDH[a7]	25 ℃	+	O_2	38.8	99
8	Au_1/CeO_2[b8]	150 ℃	-	O_2	15.9	98
9	Pt_1/CeO_2[c8]	120 ℃	-	O_2	15	90
10	$W_{18}O_{49}/ZnIn_2S_4$-60[d9]	55 ℃	+	O_2	71.5	99
11	RuOOH/ SiO*x*[e10]	35 ℃	+	O_2	92.5	Unknown
12	$Pd_{0.03}/TiO_2$[f11]	120 ℃	-	O_2	68.8	85.6
13	AuPd/TiO_2-001[g12]	120 ℃	-	O_2	85	95
14	Cs_2MoBr_6[h13]	25 ℃	+	O_2	99	97

[a]Reaction conditions: ZnTi-LDH: 20 mg; Benzyl alcohol: 0.1 mmol, Acetonitrile 1.5 ml; O_2:1 atm, $\lambda \geq 400$ nm; Reaction time: 4 hours.

[b]Reaction conditions: Catalyst: 150 mg; Benzyl alcohol: 5 mL; Reaction time: 8 hours; O_2: 0.5 Mpa; Temperature: 150 °C.

[c]Reaction conditions: Catalyst: 150 mg; Benzyl alcohol: 5 mL; Reaction time: 6 hours; O_2: 0.5 Mpa; Temperature: 120 °C.

[d]Reaction conditions: Photocatalyst: 40 mg; Benzyl alcohol: 0.2 mmol; Trifluoro Toluene: 10 mL; O_2:1 bar; $\lambda \geq 400$ nm; Reaction time: 3 hours.

[e]Reaction conditions: RuOOH/ SiO*x*: 20 mg; Benzyl alcohol: 0.444 mmol; Trifluoro Toluene: 3 mL; LED light (Fiber-Lite Mi-LED series Illuminator, Dolan-Jenner) of 965 Mw.

[f]Reaction conditions: Pd catalyst (calcination at 400 °C): 0.1 g; Benzyl alcohol: 10 mL; Pd loading (wt %): 0.03; O_2 flow rate: 90 mL/min (1 atm); Reaction time: 6 hours.

[g]Reaction conditions: catalyst mass: 30 mg; Benzyl alcohol: 15 mL; Temperature: 120 °C, O_2: 0.3 MPa; Stirring rate:1000 rpm.

[h]Reaction conditions: Catalyst mass: 10 mg; Benzyl alcohol: 0.5 mmol; Acetonitrile: 10 mL; O_2 balloon; Reaction time: 4.5 h; Xenon lamp with full-band width.

Table S2: Atom percentages (at %) of the O 1s peaks are analysed by the *in-situ* XPS of the ZnTi-LDH sample under different treated temperature at 25, 50 and 70 °C for 1h in the analysis chamber.

Entry	**Name**	25 ℃		50 ℃		70 ℃	
		Position (eV)	at %	Position (eV)	at %	Position (eV)	at %
1	Lattice oxygen	529.80	48.90	529.87	62.37	529.87	62.76
2	Oxygen Vacancy	531.85	32.90	532.00	37.63	532.02	37.87

References

1. G. Kresse, J. Hafner, *Phys. Rev. B*., 1993, **47**, 558-561.
2. G. Kresse, J. Hafner, *Phys. Rev. B*., 1994, **49**, 14251-14269.
3. J. P. Perdew, K. Burke, M. Ernzerhof, *Phys. Rev. Lett.*, 1996, **77**, 3865-3868.
4. G. Kresse, D. Joubert, *Phys. Rev. B*., 1999, **59**, 1758-1775.
5. P. E. Blöchl, *Phys. Rev. B*., 1994, **50**, 17953-17979.
6. JK. Nørskov, J. Rossmeisl, A. Logadottir, L. Lindqvist, JR. Kitchin, T. Bligaard, H. Jonsson, *J. Phys. Chem. B*., 2004, **108**, 17886–17892.
7. J. H. Zou, Z. T. Wang, W. Guo, B. B. Guo, Y. Yu, L. Wu, *Appl. Catal. B. Environ Energy*., 2020, **260**, 118185.
8. T. B. Li, F. Liu, Y. Tang, L. Li, S. Miao, Y. Su, J. Y. Zhang. J. H. Huang, H. Sun, M. Haruta, A. Q. Wang, B. T. Qiao, J. Li, T. Zhang, *Angew. Chem. Int. Ed*., 2018, **57**, 7795-7799.
9. Z. F. Yan, X. N. Xia, W. W. Yang, L. L. wang, Y. T. Liu, Appl. Catal. B. Environ Energy., 2021, 229, 120675.
10. Q. L. Wei, K. G. Guzman, X. Y. Dai, N. H. Attanayake, D. R. Stronging, Y. G. Sun, *Nano-Micro. Lett*., 2020, **12**, 41.
11. G. T. Xu, L. K. Dai, M. M. Du, A. X. Peng, G. N. Zeng, H. M. Chen, R. J. Yan, W.

Li, *ACS. Sustainable. Chem. Eng.* 2024, **12**, 2751-2760.

12. Z. Wang, J. J. Feng, X. L. Li, R. N. Oh, D. D. Shi, O. Akdim, M. Xia, L. Zhao, X. Y. Huang, G. J. Zhang, *J. Colloid. Interf. Sci*., 2021, **588**, 787-794.
13. Q. K. Kong, X. C. Wang, B. Y. Liu, J. Lava, M. A. M. Parent, J. S. Chen, Feng, Y. Y. Feng, F. Liu, *Chem. Eng. J*., 2025, **514**, 163152.